Research Article

Journal of Environmental Nanotechnology

Experimental Analysis of Nanofluid Circulation in Automobile Radiators: Thermal Efficiency and Flow Behaviour

G. D. Gosavi[1*], P. Sivamurugan[1], Mohamed Iqbal Shajahan[1] and Bharathiraja[2]

[1]Department of Mechanical Engineering, Vel Tech Rangarajan Dr. Sagunthala R&D Institute of Science and Technology, Chennai, TN, India
[2]Centre for Additive Manufacturing, Chennai Institute of Technology, Chennai, TN, India
Received: 16.04.2025 Accepted: 11.06.2025 Published: 30.09.2025
*gdgicoer@gmail.com

ABSTRACT

The heat transfer of coolant advancement through radiators significantly influences the optimization of fuel consumption in automobiles. In order to cool the circulating fluid, which is typically water or a water-based mixture, forced convection heat transfer is employed in automotive radiators. This study experimentally assessed the heat-transfer performance of an automobile radiator by evaluating the thermal performance of a specially prepared nanofluid. The nanofluid was created using a two-step process, involving demineralized water enhanced with graphene (GPN) nanoparticles at concentrations of 0.1 and 0.5 vol. %, along with the addition of GPN to cetyltrimethylammonium bromide (CTAB) surfactant in a 1:0.5 ratio for extended stability at the same concentrations. The experiments varied the liquid-side Reynolds number from 10,000 to 27,000, keeping the radiator inlet liquid at a constant temperature of 60-80 °C. This study thoroughly examined the impact of these variables on the overall heat-transfer coefficient. The experimental results show that the maximum increases in both thermal conductivity ratio and viscosity ratio were 32% and 144% without surfactant, and 33% and 165% with the addition of CTAB surfactant. The maximum average increases in the Nusselt number were 18.55% and 26.49% for the GPN/water nanofluid, and 49.05% and 57.56% for the GPN-CTAB/water nanofluid, respectively. The highest performance evaluation criteria relative to the Reynolds number using the GPN/water nanofluid at concentrations of 0.1 and 0.5 vol. % were recorded as 1.30 and 1.29, while for the GPN-CTAB/water nanofluid, the performance values were 1.14 and 1.10. Furthermore, the findings confirm that incorporating nanoparticles and surfactants into the base fluid results in superior performance compared to using water alone.

Keywords: Nanofluids; Graphene; Sustainability; Phase change material; Heat transfer.

1. INTRODUCTION

A radiator is a condensed heat exchanger employed to dissipate surplus heat produced by internal combustion engines through the circulation of coolant. The engine cooling system uses a coolant to remove about 30% of the engine's heat that would otherwise escape through the radiator into the atmosphere. As modern engines continue to grow in power, traditional coolants are no longer adequate for meeting the increased heat dissipation demands of cooling systems. There is an urgent need to develop more efficient heat transfer coolants. The advent of nanofluid technology offers novel approaches for enhancing heat transfer rates (Li *et al*. 2020; Ahmadi *et al*. 2020; Ruey *et al*. 2022; Kumar *et al*. 2023).

The most frequently utilized radiator coolants are water and ethylene glycol, but their energy transfer abilities are constrained by their chemical composition and thermophysical properties. In recent decades, numerous studies have explored various methods to improve heat transfer rates, including microchannels, engineered surface texturing, twisted tape inserts, and diverse fin designs (Abderezzak and Randi, 2020; Sundari *et al*. 2021). Nevertheless, these conventional approaches for enhancing cooling rates have faced certain obstacles. Heat transfer plays a crucial role in many industrial applications (Hosain *et al*. 2019; Kumar *et al*. 2020; Kohne *et al*. 2021; Miao *et al*. 2023). Consequently, there is a need for innovative and advanced heat transfer fluids to boost the heat transfer rate in automotive radiators.

Nanofluids have emerged as promising alternatives to traditional coolants in engine cooling systems (Fu *et al*. 2023). Nanoparticle suspended fluids display good thermal properties. Nanofluids are colloidal suspension mixtures of a base fluid with metallic or non-metallic nano-sized particles typically having a size <100 nm in at least one dimension. Uniformly suspended particles enable them to exhibit improved thermal properties, which can lead to more efficient heat transfer in the heat exchanger (Zakaria *et al*. 2022; Ferrão *et al*. 2022).

Present studies focus on clarifying the complex interactions between nanoparticle properties and their influence on nanofluid performance. This advanced knowledge enables the design of precisely engineered nanofluids, allowing customized thermal solutions to address specific challenges in thermal management and heat-transfer applications. Recent studies focus on many nanomaterials dispersed in base fluids (Bigdeli *et al*. 2016). These nanomaterials fall under three separate classifications namely, metal oxides, metallic nanoparticles, and carbon-based compounds (Lawal *et al*. 2023). Achieving desired results in thermal-fluid systems depends on the correct selection of nanofluids. The convective heat transfer properties of nanofluids made of aluminum oxide, copper, carbon nanotubes (CNTs), graphene, and copper oxide (Abdullatif *et al*. 2023) have been extensively researched on. Often, the volumetric concentration of nanoparticles in these fluids is under 5%. Ravi *et al*. (2020) undertook an experimental investigation of the stability and thermophysical characteristics of ethylene glycol (EG) based nanofluids. Their study showed that a nanofluid including multi-walled carbon nanotubes (MWCNTs) in an 80:20 ratio of ethylene glycol to water reached a maximum thermal conductivity increase of 26%. Chandrasekaran *et al*. (2022) synthesized nanofluids by adding varying amounts of cerium oxide nanoparticles into a base fluid composed of water and EG in a 3:2 ratio. The researchers discovered that an increase in flow velocity and volume concentration of the nanofluid correspondingly elevated the heat transfer rate. Furthermore, their findings indicated that under specific conditions, the Nusselt number and heat transfer rate reached maximum of 13.39 and 6.2%, respectively.

(Arunkumar *et al*. 2019) examined the efficacy of car radiators utilizing a mixture of EG and water, together with nanoparticles of aluminum oxide, magnesium oxide, and titanium dioxide as cooling agents. They employed a ratio of 20:80 for ethylene glycol to water and dispersed the nanoparticles at two specific concentrations (0.12% and 0.4%). Their findings demonstrated a direct correlation among three variables (air velocity, nanofluid velocity, and nanoparticle concentration) and the overall heat transfer coefficient.

(Arshad and Ali, 2017) prepared a water-based nanofluid containing titanium dioxide (TiO_2) for the thermal performance and pressure drop study inside a narrow channel heat sink. Their analysis discovered a negative relationship between heating power and pressure drop where the pressure drops increased as the heating power decreased. Interestingly, this effect was more prominent when using the TiO_2 nanofluid instead of pure water.

(Ijaz *et al*. 2020) developed a simulation-based study on the thermal properties of a graphene-doped nano coolant in a car radiator. The work focused on a particular section of the radiator constructed using Solid-Works software. The CFD study ran ANSYS Fluent module. The work looked at how graphene oxide nanoparticles mixed with water as a base fluid influenced the temperature decrease down the tube and the overall performance of the car radiator.

(Nieh *et al*. 2014) prepared Al_2O_3 and TiO_2 nanoparticles distributed in EG-water that could increase the thermal performance of an air-cooled radiator system. To analyze heat transfer rate, pumping power, pressure drop, and efficiency factor, the researchers undertook experiments with various volumetric flow rates, temperatures, and volume fractions. Their findings revealed that both nano-coolants outperformed the EG-water mixture in heat transfer capacity and efficiency, with the TiO_2 based nano-coolant outperforming the Al_2O_3 based nano-coolant. The nano-coolants outperformed the EG-water mixture by 25.6% in heat transfer capacity, 6.1% in pressure drop, 2.5% in pumping power, and 27.2% in efficiency. However, very minimal increase in pressure drop and pumping power were observed.

Several studies indicated that the thermal conductivity of the nanofluid increased with increasing temperature. Based on lubricating oil, (Kole and Dey, 2011) looked at how the thermal conductivity of a CuO nanofluid varied with fluid temperature. Their work revealed that a nanofluid with a 2.5% volume percentage greatly enhanced thermal conductivity, by 10% at 30 °C and 12% at 80 °C, respectively. (Jeong *et al*. 2016) investigated the viscosity of Zinc Oxide (ZnO) nanofluids comprising nanoparticles of diverse shapes, including spherical and almost rectangular particles, at various volumetric concentrations. The viscosity increased significantly with particle concentration; for the roughly rectangular particles, it varied from 5.3% to 68.6% and for the spherical ones, it was 5.9% to 59.0%, with concentrations ranging from 0.5 vol% to 5.0%.

In the current study, graphene nanoplatelets (GNP) were selected for their exceptionally high in-plane thermal conductivity (≈ 3000–5000 W m K^{-1}) and their two-dimensional morphology, which allows the formation of a percolating thermal-conduction network at loadings below 0.1 wt %. At these ultralow concentrations water-based GNP nanofluids routinely deliver 12–28 % enhancements in thermal conductivity, that is more than double the gains reported for oxide (Al_2O_3, TiO_2) or metal nanoparticles under identical conditions, which typically require order-of-magnitude higher loadings to achieve single-digit improvements. Also, cetyltrimethylammonium bromide (CTAB) was chosen as the dispersant because its cationic head group adsorbs strongly onto graphitic surfaces, creating an electrostatically charged bilayer that suppresses platelet restacking and Brownian aggregation. At its critical micelle concentration, CTAB maintains dispersion

stability up to 70 °C with performance that clearly surpasses anionic surfactants such as SDS or SDBS, which give lower zeta potentials and shorter stability windows.

This paper outlines the experimental analysis of the convective heat transfer coefficient in forced convection for four different fluids, benchmarked against pure water. Graphene nanoplatelets nanofluids at various volume concentrations (0.1, and 0.5, vol. %), incorporating the CTAB surfactant (to enhance stability) were investigated. The influence of operational parameters on the heat transfer performance of a radiator using nanofluids was assessed. The GNP nanoparticles were chosen for their moderate thermal conductivity compared to metal oxides like Al_2O_3 and CuO_2.

The findings confirm that the hydrophobic characteristics of GPN nanoparticles boost the efficiency of the radiator's forced convection system. While conventional nanofluids often require higher concentrations (typically >1 vol.%) of metal or metal oxide nanoparticles to yield modest performance gains, GNPs can deliver comparable or superior enhancements at lower loadings, reducing issues such as increased viscosity, sedimentation, and energy penalty in pumping.

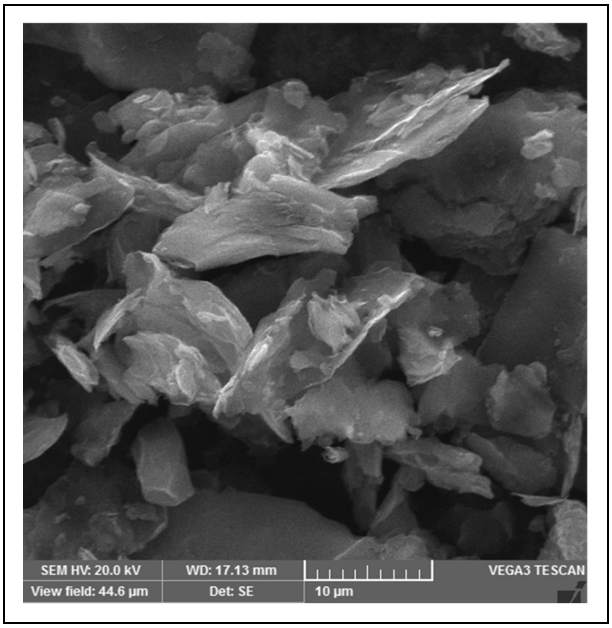


Fig. 1: SEM image of GPN

2. MATERIALS AND METHODS

2.1 Preparation of GPN Nanofluid

The nanofluid materials studied in this paper comprised of demineralized water and GPN nanoparticles (Table 1). Graphene nanoplatelets nanoparticles were purchased from Sigma-Aldrich company.

The thermal performance of GPN-based nanofluids is highly dependent on the morphological characteristics of the nanoparticles, particularly their lateral size, thickness, and aspect ratio. These parameters directly impact the mechanisms of heat conduction, dispersion stability, and dynamic interactions within the base fluid. The surface morphology and microstructures of GPN nanoparticles were studied with a scanning electron microscope (SEM, Nova Nano SEM; Fig. 1).

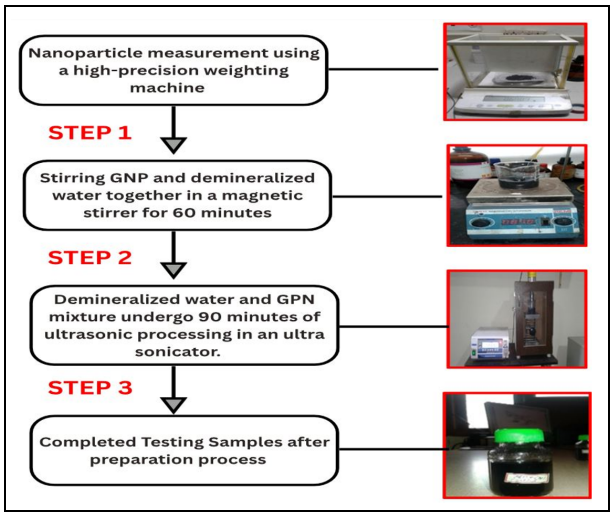


Fig. 2: Flow chart of nanofluid preparation process

Table 1. Thermophysical properties of DI and nanomaterial

Property	DI	Graphene
Particle Size (nm)	-	50
Density, kg/m^3	997	2600
Specific heat, J/kg K	4220	710
Thermal conductivity, W/mK	0.606	5300

Nanofluids were prepared using demineralized water with various volume fractions (0.1% and 0.5%) of GPN nanoparticles. Volumetric concentration for the amount of GPN nanoparticles required was determined using Eq. (1).

$$\text{Volume concentration, } \varphi = \left[\frac{\frac{W_{Particle}}{\rho_{Particle}}}{\frac{W_{Particle}}{\rho_{Particle}}+\frac{W_{fluid}}{\rho_{fluid}}}\right] \times 100 \qquad \ldots (1)$$

A two-step process was employed to prepare GPN/demineralized water nanofluids with volume fractions (0.1% and 0.5%) of GPN nanoparticles combined with deionized water. A high-precision digital scale was utilized for weighing materials, with initial mass calculations based on the density of the nanoparticles. Following the addition of the nanoparticles to water, the mixture underwent magnetic stirring for approximately 60 min at 450 rpm. Subsequently, the suspensions were subjected to ultrasonic processing (500 W, 20 kHz) for approximately 90 minutes. The ultrasonic processing ensured disruption

of particle aggregates, prevention of sedimentation, uniform particle distribution and suspension stability. The preparation process of the GPN/water nanofluids is illustrated in Fig 2. To ensure the uniformity and stability of the GPN nanofluid, cationic CTAB was employed as the surfactant in addition with nanoparticles in the ratio of 1:0.5 (GPN: CTAB) at 0.1 and 0.5 vol.% with the same concentration. Four different nanofluids were prepared and compared to the base fluid water. Minimal change was noticed in visual clarity, with no significant sediment formation even after 50–100 cycles. Stable zeta potential values (typically > +50 mV) were indicative of strong electrostatic stabilization.

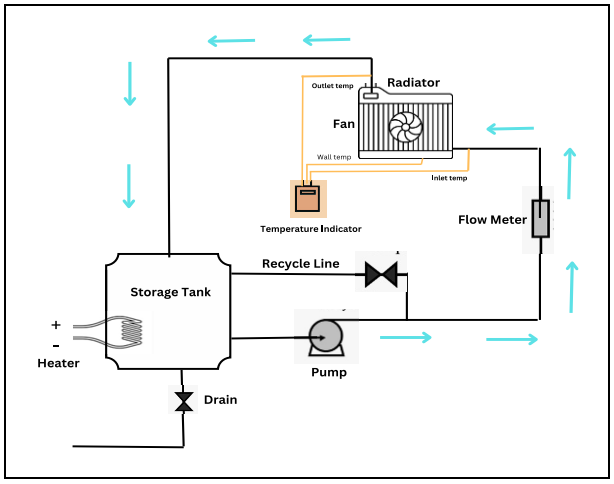


Fig. 3: Experimental setup

2.2 Experimental setup and procedure

Fig. 3 shows the experimental test rig that consisted of a plastic reservoir tank (50 cm high and 40 cm wide), an electric heater with a power of 2000 W, eight K-type thermocouples for temperature measurement, a DC power supply (0-15 V), a fan, two valves, plastic tubes (diameter = 0.5 in), a flowmeter with a range of 0-500 LPH, a centrifugal pump with a 0.5 hp motor and a heat exchanger (automobile radiator). The electric heater was installed inside the plastic reservoir tank to heat up the coolant to the desired temperature. A voltage regulator was used to regulate the power supply to the heater to maintain the temperature in the radiator within the range of 60-80 °C. Two valves and a flowmeter were employed to control and measure the flow rate of the coolant, respectively. The total volume of the circulating coolant was kept constant at 4 L throughout the experiment. To record the outlet and inlet temperatures of the coolant, two K-type thermocouples were connected to the flow line. Also, six K-type thermocouples were attached to the radiator surface to measure the surface temperature. The pressure drop at the inlet and outlet of the radiator was measured using a U-tube mercury manometer. Before conducting the experiments, the temperature recorder, anemometer and thermocouples were calibrated to ensure accurate measurements.

2.3 Error Analysis

The measurement of uncertainty refers to the estimated interval in which the actual value of a measured quantity is anticipated to exist. It originates from several elements such as constraints of the measurement instrument, ambient circumstances, and human participation. Including uncertainty in measurement is necessary to evaluate the reliability and validity of outcomes. The uncertainty is calculated using equation and accuracies of 0.75% (measured temperature) +1.5 °C and ±0.01% of full-scale flow rate +2.5% (measured value) was associated with the thermocouples and flow meter.

$$\partial R = \sqrt{(\frac{\partial R}{\partial x_1} w_1)^2 + (\frac{\partial R}{\partial x_2} w_2)^2 + \cdots + (\frac{\partial R}{\partial x_n} w_n)^2} \quad \ldots (2)$$

2.4. Data reduction

2.4.1 Estimation of heat transfer coefficient

The coefficient of heat transfer and corresponding Nusselt number in the radiator were determined using following procedure. According to Newton's cooling law (Pak *et al.* 1998),

$$Q = hA\Delta T = hA(T_B - T_w) \quad \ldots (3),$$

where,

$$T_B = \frac{T_{in}+T_{out}}{2} \quad \ldots (4)$$

$$T_w = \frac{T_1+T_2+T_3+T_4+T_5+T_6+T_7+T_8}{8} \quad \ldots (5)$$

Rate of heat transfer was determined as follows:

$$Q = mC_p\Delta T = mC_p(T_{in} - T_{out}) \quad \ldots (6)$$

Estimation of Nusselt number by collecting Eqs. (6) and (7):

$$Nu = \frac{h_{expt} \times d_{hyd}}{k} = \frac{\dot{m}C_p(T_{in}-T_{out})}{A(T_B-T_W)} * \frac{d_{hyd}}{k} \quad \ldots (7),$$

Where,

$$\dot{m} = \rho * \dot{V} \quad \ldots (8)$$

Reynolds number (Re) was determined as:

$$Re = \frac{\rho * d_{hyd} * u}{\mu} \quad \ldots (9)$$

Where,

$$u = \dot{V}\, n * Ac \quad \ldots (10)$$

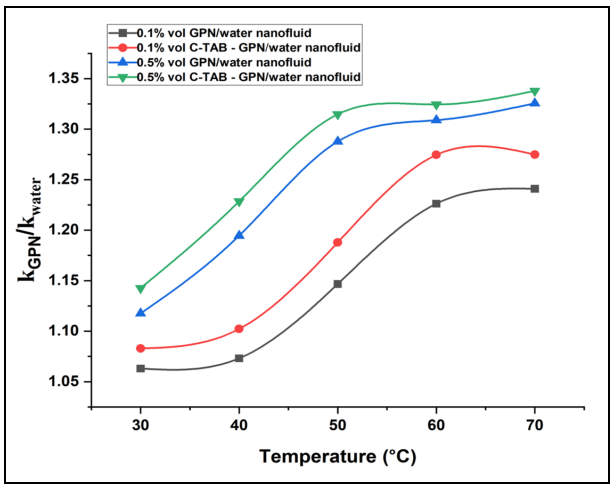


Fig. 4: Thermal conductivity ratio for different GPN combinations

3. RESULTS AND DISCUSSION

3.1 Thermo-Physical Properties

Fig. 4 illustrates the enhancement ratio of thermal conductivity in nanofluids compared to water, plotted against temperature, both with and without the surfactant CTAB (k_{Nf}/k_{bf}), where k_{Nf} represents the thermal conductivity of nanofluids and k_{bf} denotes the thermal conductivity of pure water. An increase in thermal conductivity values with rising temperature and GPN concentration was noted. Specifically, the thermal conductivity enhancement ratio of nanofluids at 0.1 vol. % GPN increased from 6.30 % to 24.09 % as the temperature increased from 30 °C to 70 °C. These findings suggest that incorporating GPN into water suspensions significantly boosts thermal conductivities when CTAB surfactant is present. The measured thermal conductivity values of nanofluids containing GPN and GPN/CTAB increased with higher volume concentrations. The incorporation of CTAB, plays a crucial role in modifying the physicochemical properties of the GNP-based nanofluid. CTAB not only stabilizes the nanofluid but also optimizes its thermal and rheological behaviour, making it suitable for use in heat transfer and cooling systems.

The experimental data revealed substantial increases in the conductivity ratio of the GPN/water nanofluid at 30 °C, with increases of 6.3 % and 13.76 % at 0.1 vol. % and 0.5 vol. %, respectively. Nanofluids with a 1:0.5 ratio of GPN/CTAB showed even greater thermal conductivity enhancements, reaching 24.09 % at 0.1 vol. % and 32.56 % at 0.5 vol. %. At a higher temperature of 70 °C, the GPN/water nanofluid exhibited conductivity increases of 24.79% and 32.59% at concentrations of 0.1 and 0.5 vol. %, respectively. Under the same conditions, the CTAB GPN/water nanofluid demonstrated further increases of 27.48 % and 33.79 % for the same concentrations.

The thermal conductivity showed improvement of the nanofluid as a function of temperature at two different GPN volume percentages with water, similarly with the surfactant graphene: CTAB added in a 1:0.5 ratio. As shown, the thermal conductivity values of nanofluids with a (1:0.5) ratio were slightly higher than those with a (1:0.5) ratio at the same GPN concentration. This enhancement in thermal conductivity can be attributed to several mechanisms, including Brownian motion, nano-clustering, and ballistic phonon motion. It is confirmed that the addition of CTAB surfactant leads to increased thermal conductivity; however, the viscosity was also carefully evaluated when the surfactant was added, as it affects the pumping power, ensuring that the nanofluid with surfactant is suitable for heat transfer applications.

Fig. 5 illustrates the viscosity ratio at elevated shear rates, calculated by dividing the viscosity of the GPN/water nanofluid by that of the base fluid at the same shear rates, across temperatures from 30 °C to 70 °C in increments of 10 °C. Despite the strong temperature dependence observed in both nanofluids and base fluids, the viscosity ratio consistently exceeded for all tested nanofluid temperatures.

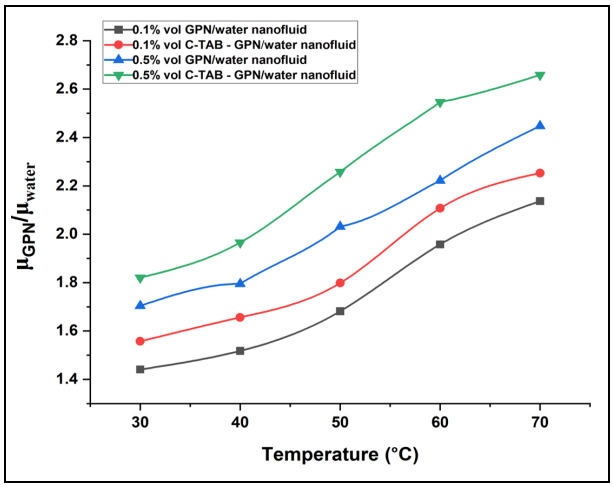


Fig. 5: Viscosity ratio for different GPN combinations

The experimental results reveal notable increases in the dynamic viscosity of the GPN/water nanofluid at 30 °C, with increases of 44.09% and 70.42% at 0.1 vol. % and 0.5 vol. %, respectively. Nanofluids with a GPN/CTAB ratio of 1:0.5 showed even greater viscosity enhancements, reaching 57.70% at 0.1 vol. % and 82.02% at 0.5 vol. %. At a higher temperature of 70 °C, the GPN/water nanofluid exhibited viscosity increases of 118.63% and 144.79% at concentrations of 0.1 and 0.5 vol. %, respectively. Under the same conditions, the CTAB GPN/water nanofluid demonstrated further increases of 121.28% and 165.84% for the same concentrations. An increase in viscosity caused by adding GPN nanoflakes at 0.1 and 0.5 vol. % to water, as well as GPN nanoflakes at the same

concentrations combined with CTAB in a 1:0.5 ratio was noted. As the nanofluid's temperature rises from 30 to 70 ℃, the dynamic viscosity ratio of GPN/water nanofluids at 0.1 and 0.5 vol. % mirrors the increase seen in GPN-CTAB/water at identical concentrations. The rise in the dynamic viscosity ratio (μnf/μbf) with the nanofluid's temperature can be linked to the decrease in dynamic viscosity of the nanofluid with smaller particles compared to pure water. This study thoroughly explored how volume fraction affects the increase in nanofluid viscosity ratio, taking into account the geometry of the nanoflakes and the addition of CTAB surfactant to reduce agglomeration. The clustering of nanoparticles can result in increased viscosity. Ultimately, the viscosity of nanofluids is affected by several factors, including the type, size, and shape of the nanoparticles, surfactants, and the viscosities of the base fluids.

3.2 Heat Transfer to Pure Water (Validation of Experimental Setup)

In a controlled testing environment, multiple experimental runs were conducted, and the results were assessed against established empirical correlations to confirm the accuracy and dependability of the instruments. The experimentally determined Nusselt number and friction factor were rigorously compared with the standard correlations derived from the Dittus-Boelter (1930) equation. The outcomes for the uniformly heated pipe under turbulent flow conditions remained within a permissible range. The standard correlations for the Nusselt number were obtained by the following equation (Tam and Ghajar, 2006),

$$Nu = 0.023Re^{0.8} Pr^{0.4} \quad \ldots (11)$$

Fig. 6 illustrates the relationship between the Nusselt number and the Reynolds number, as derived from both experimental data and the Dittus-Boelter correlation for the test section. A detailed examination revealed that the experimentally evaluated values deviated by approximately 8.3% when compared to the theoretical values.

The standard correlations for the friction factor were obtained by the following equation (Gnielinski 1976),

$$f = 0.316/Re^{0.25} \quad \ldots (12)$$

Fig. 7 depicts the variation of friction factor and Reynolds number for the experimental values and estimated values for Blasius correlation are presented. It was noted that the evaluated experimental values lie with deviations of ±8.9% than the theoretical values.

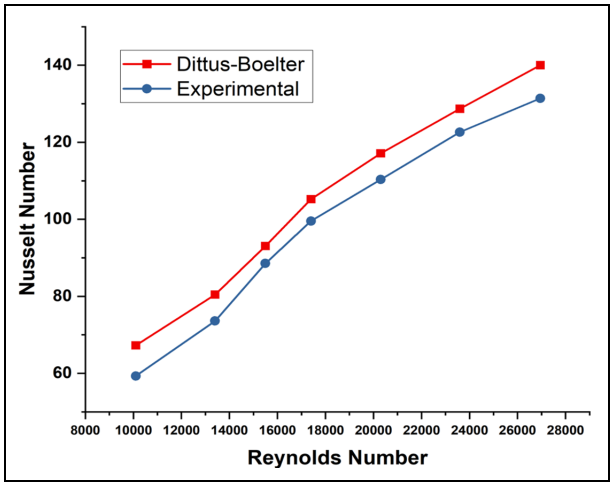


Fig. 6: Validation of experimental Nusselt number for plain tube under turbulent flow

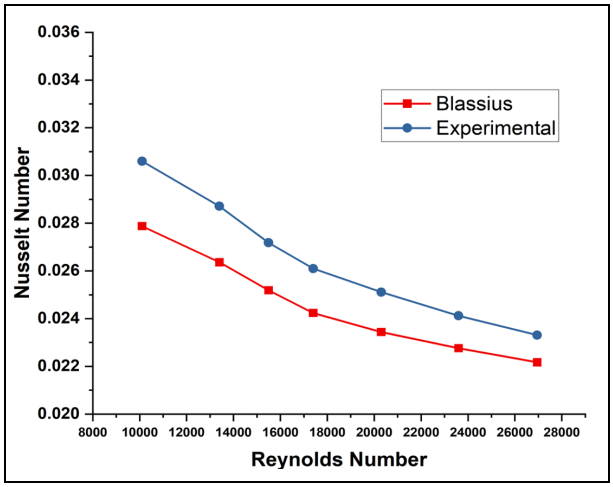


Fig. 7: Validation of experimental frictional power for plain tube under turbulent flow

3.1 Heat Transfer Study

Fig. 8 depicts the trends of the Nusselt number in relation to the Reynolds number for GPN/water nanofluids at 0.1 and 0.5 vol. %, as well as GPN-CTAB/water nanofluids at 0.1 and 0.5 vol. %, utilized as working fluids in a radiator for a closed-loop forced convection system. It was observed that the Nusselt number increases with an increase in particle volume concentration and also with an increase in Reynolds number. The maximum average increases in the Nusselt number were 18.55% and 26.49% for GPN/water at 0.1 and 0.5 vol. %, respectively. In contrast, the GPN-CTAB/water nanofluid at 0.1 and 0.5 vol. % exhibited average Nusselt number increases of 49.05% and 57.56%, respectively, compared to water alone over the range of Reynolds numbers (Roy *et al*. 2024).

The nanofluids enhanced the convective heat transfer rate due to augmented thermal conductivity and

ballistic phonon motion. The addition of CTAB significantly influenced heat transfer enhancement, as the suspension and surface charges of the nanoparticles within the fluid (specifically the stability of the GPN-CTAB/water nanofluid) resulted in superior heat transfer performance compared to the GPN/water nanofluid (evidenced by a larger gap in the curve trend). This finding aligns with the previously discussed thermal conductivity ratio.

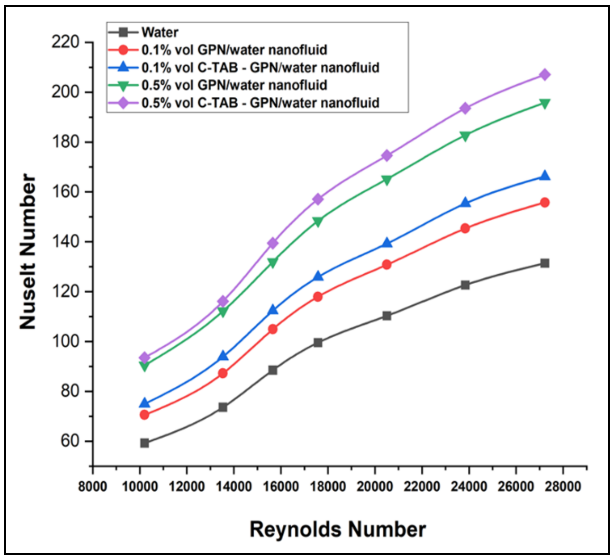


Fig. 8: Heat transfer study of GPN combination

Table 2. Summary of various GPN Nanofluid studies

Ref	Nanofluid Type	Thermal Conductivity Ratio	Max Nusselt Nu
Arunkumar *et al.* (2019)	Al_2O_3–water	1.08	110
Jeong *et al.* (2013)	ZnO–water	1.20	-
Kole and Dey, (2011)	Cuo- Gear oil	1.13	125
Li *et al.* (2021)	Hy MWCNTs - Water	1.12	110.85
Present Study	GPN - Water	1.33	155-207

The convective heat transfer coefficient (h) is dependent on k/dt, where k represents thermal conductivity and dt denotes tube diameter. The convective heat transfer coefficient (h) increases with an increase in effective thermal conductivity k and decreases with an increase in tube diameter (Akshay *et al.* 2024). The GPN and CTAB-GPN disrupt the thermal boundary layer of the fluid through the radiator tubes, leading to an enhancement in the heat transfer coefficient, and consequently, the Nusselt number. The heat transfer mechanism in GPN nanofluids is governed by:

- Intrinsic high thermal conductivity of GPNs.
- Percolation network formation enabling direct heat conduction paths.
- Brownian motion-driven micro convection, contributing to dynamic energy transport.
- Minimized agglomeration, preserving the nanoplatelets' effective surface area.

Comparative studies of different combinations of carbon based nanofluid in the heat transfer is summarised in the Table 2.

3.4 Pressure Drop Study

The relationship between the friction factor and the Reynolds number is clearly depicted in Fig. 9. A thorough analysis indicates that utilizing GPN/water nanofluid at concentrations of 0.1 and 0.5 vol. %, along with GPN-CTAB/water nanofluid at identical concentrations in a radiator leads to a greater friction factor than when using only water. The friction factor escalates with an increase in volume concentration and declines as the Reynolds number rises. For the GPN/water nanofluid, the friction factor increases by approximately 26.50% and 37.18% for 0.1 and 0.5 vol. %, respectively.

Conversely, the GPN-CTAB/water nanofluid exhibits a maximum increase of about 67.74 and 77.80 % for the same concentrations. The addition of a surfactant results in higher viscosity compared to using water alone, which slightly elevates the pumping power. This finding is consistent with the viscosity ratio. Furthermore, it was observed that the friction factor diminishes with an increase in the Reynolds number due to the enhanced momentum of the fluid. The interaction of particles with the wall region enhances convective heat transfer and simultaneously increases the pressure drop due to the higher viscosity compared to water. The variation in trends between GPN with and without surfactant is due to the improved stability of the nanofluid when a surfactant is added (Ijaz *et al*. 2020).

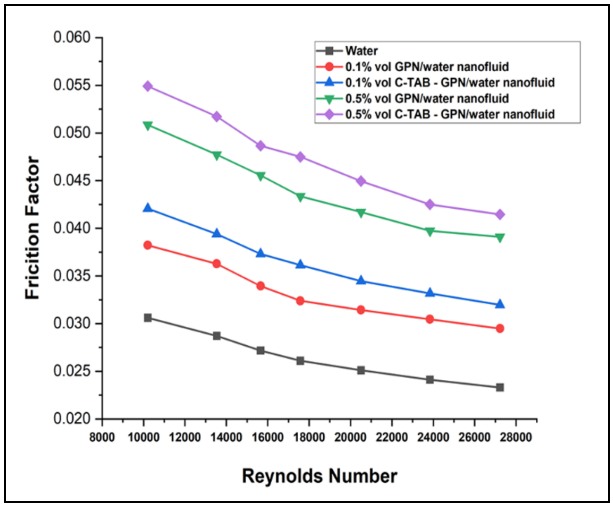


Fig. 9: Pressure drop study of GPN combination

3.5 Performance Evaluation Criteria (PEC)

The impact of GPN/water and GPN-CTAB/water on enhancing heat transfer (linked to an increase in pressure drop) was assessed using a metric known as the thermal performance evaluation criteria (PEC). This metric incorporates the Nusselt number and friction factor to evaluate heat-transfer improvement and pressure-drop characteristics, respectively. This index is utilized to determine the radiator efficiency of the graphene-based nanofluid. The thermal performance factor is defined as the ratio of the Nusselt number ratio to the friction factor ratio when pumping powers are equal, as shown in equation 13

$$PEC = \frac{\frac{Nu}{Nu_p}}{\left(\frac{f}{f_{pt}}\right)^{0.33}} \quad \ldots (13)$$

Fig 10 depicted the variations in performance evaluation criteria relative to the Reynolds number using GPN/water nanofluid at concentrations of 0.1 and 0.5 vol. %, as well as GPN-CTAB/water nanofluid at the same concentrations. It was noted that the performance evaluation criteria exceeded unity, and the graph highlighted the combined impact of heat transfer and flow resistance within the radiator. The highest performance evaluation values were recorded as 1.30 and 1.29 for the GPN-CTAB/water nanofluid and GPN/water nanofluid at 0.5 vol. %, respectively. In contrast, at 0.1 vol. %, the performance values were 1.14 and 1.10. It was deduced that a higher Reynolds number provided a favorable swirl flow intensity, thereby enhancing the thermal performance factor in the presence of the surfactant in the GPN nanofluid. Furthermore, the findings confirm that incorporation of nanoparticles and surfactants into the base fluid yields better performance than using water alone.

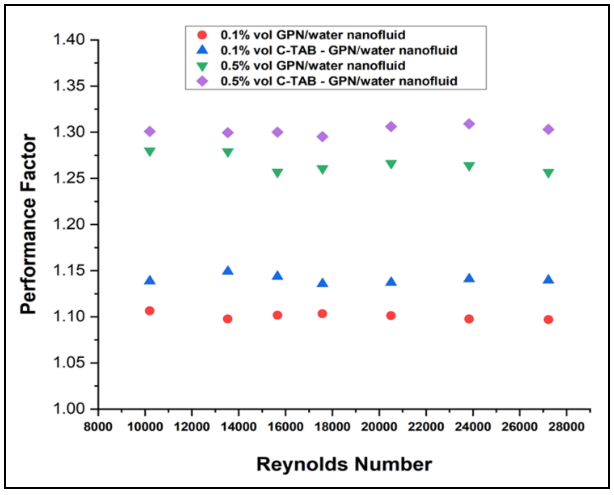


Fig. 10: PEC of GPN combination

4. CONCLUSION

This study investigated the formulation, stability, and thermophysical behaviour of GPN nanofluids, focusing on thermal conductivity, viscosity, and heat-transfer performance. Nanofluids with 0.1 and 0.5 vol.% concentrations were prepared using a two-step method and evaluated across 30–70 °C. The results showed that thermal conductivity increased with concentration, reaching enhancements of 24.79% and 32.59% for GPN/water and 27.48% and 33.79% for CTAB-GPN/water at 70 °C. Viscosity ratios (μ_nf/μ_bf) also rose with temperature and concentration, with GPN/water showing increases of 118.63% and 144.79% and CTAB-GPN/water showing 121.28% and 165.84% at 70 °C. Heat-transfer analysis revealed that the Nusselt number increased with Reynolds number, achieving maximum enhancements of 18.55% and 26.49% for GPN/water and 49.05% and 57.56% for CTAB-GPN/water. The friction factor similarly increased, by 26.50% and 37.18% for GPN/water and by 67.74% and 77.80% for CTAB-GPN/water. Overall, the performance evaluation criterion demonstrated strong heat-transfer performance, with values of 1.30 and 1.29 for GPN/water and 1.14 and 1.10 for CTAB-GPN/water at 0.1 and 0.5 vol.%, respectively.

ACKNOWLEDGEMENT

The authors extend their appreciation towards Dr. Saravanan, National College Instrumentation Facility (NCIF), National College, Tiruchirapalli, India, for his support to carry out characterization work involved in this research study.

FUNDING

This research received no specific grant from any funding agency in the public, commercial, or not-for-profit sectors.

CONFLICTS OF INTEREST

The authors declare that there is no conflict of interest.

COPYRIGHT

This article is an open-access article distributed under the terms and conditions of the Creative Commons Attribution (CC BY) license (http://creativecommons.org/licenses/by/4.0/).

REFERENCES

Abderezzak, B. and Randi, S., Experimental investigation of waste heat recovery potential from car radiator with thermoelectric generator, *Therm. Sci. Eng. Prog.*, 20100686 (2020). https://doi.org/10.1016/j.tsep.2020.100686

Abdullatif, A. L., Shaik, F. and Syam, S. L., Thermal efficiency enhancement of mono and hybrid nanofluids in solar thermal applications – A review, *Alex. Eng. J.*, 68365–404 (2023). https://doi.org/10.1016/j.aej.2023.01.043

Ahmadi, M. H., Ghazvini, M., Maddah, H., Kahani, M., Pourfarhang, S., Pourfarhang, A. and Heris, S. Z., Prediction of the pressure drop for CuO/(Ethylene glycol-water) nanofluid flows in the car radiator by means of Artificial Neural Networks analysis integrated with genetic algorithm, *Phys. Stat. Mech. Its Appl.*, 546, 124008 (2020). https://doi.org/10.1016/j.physa.2019.124008

Akshay, J., Vinayak, K., Banapurmath, N. R., Prasanna, S. R., Ashok, M. S., Yunus, K. T. M., Ayachit, N. H., Irfan, A. B., Experimental and numerical investigation of heat transfer characteristics of radiator using Graphene Amine-based nano coolant, *Case Stud. Therm. Eng.*, 63 105389, (2024). https://doi.org/10.1016/j.csite.2024.105389

Arshad, W. and Ali, H. M., Experimental investigation of heat transfer and pressure drop in a straight minichannel heat sink using TiO2 nanofluid, *Int. J. Heat Mass Transf.*, 110248–256 (2017). https://doi.org/10.1016/j.ijheatmasstransfer.2017.03.032

Arunkumar, T., Anish, M., Jayaprabakar, J. and Beemkumar, N., Enhancing heat transfer rate in a car radiator by using $Al_2 O_3$ nanofluid as a coolant, *Int. J. Ambient Energy*, 40(4), 367–373 (2019). https://doi.org/10.1080/01430750.2017.1392356

Bigdeli, M. B., Fasano, M., Cardellini, A., Chiavazzo, E. and Asinari, P., A review on the heat and mass transfer phenomena in nanofluid coolants with special focus on automotive applications, *Renew. Sustain. Energy Rev.*, 601615–1633 (2016). https://doi.org/10.1016/j.rser.2016.03.027

Chandrasekaran, M., Prakash, K.B., Subramaniyan, C., Santhosh, N. and Tamilarasan, V.D., Experimental investigation on heavy duty engine radiator using cerium oxide nano fluid, *Mater. Today, Proc.*, 661497–1500 (2022). https://doi.org/10.1016/j.matpr.2022.06.284

Ferrão, T. A. L. O., Henríquez, J .R., Da, C. J. Â. P. and Abramchuk, V., Comparative performance analysis of internal combustion engine water jacket coolant using a mix of Al2O3 and CuO-based nanofluid and ethylene glycol, *Energy*, 250123832 (2022). https://doi.org/10.1016/j.energy.2022.123832

Fu, X., El-Rahman, M. A., Abdalla, A. N., Hasani, M. E. and Sharifpur, M., The numerical analysis and optimization of a Photovoltaic thermal collector with three different plain, ribbed, and porous-ribbed absorber tubes and a nanofluid coolant using two-phase model, *J. Taiwan Inst. Chem. Eng.*, 148, 104725 (2023). https://doi.org/10.1016/j.jtice.2023.104725

Gnielinski, V., Turbulent Pipe and Channel Flow, *Int. Chem. Eng.*, 16(2), 359-368 (2013).

Hosain, M. L., Domínguez, J. M., Bel Fdhila, R. and Kyprianidis, K., Smoothed particle hydrodynamics modeling of industrial processes involving heat transfer, *Appl. Energy*, 252, 113441 (2019). https://doi.org/10.1016/j.apenergy.2019.113441

Ijaz, H., Raza, H., Gohar, G. A., Ullah, S., Akhtar, A. and Imran, M., Effect of graphene oxide doped nano coolant on temperature drop across the tube length and effectiveness of car radiator – A CFD study, *Therm. Sci. Eng. Prog.*, 20, 100689 (2020). https://doi.org/10.1016/j.tsep.2020.100689

Jeong, C. J., Lee, G., In, I. and Park, S. Y., Concentration-mediated multicolor fluorescence polymer carbon dots, *Luminescence*, 31(3), 897–904 (2016). https://doi.org/10.1002/bio.3050

Kole, M. and Dey T. K., Role of interfacial layer and clustering on the effective thermal conductivity of CuO-gear oil nanofluids, *Exp. Therm. Fluid Sci.,* 35(7), 1490–1495 (2011). https://doi.org/10.1016/j.expthermflusci.2011.06.010

Kohne, T., Burkhardt, M., Theisinger, L. and Weigold, M., Technical and digital twin concept of an industrial heat transfer station for low exergy waste heat, *Procedia CIRP*, 104, 223–228 (2021). https://doi.org/10.1016/j.procir.2021.11.038

Kumar, A., Chand, P. and Hassan, M.A., Louvered finned car radiator with MWCNT-SiO2 hybrid nanofluid: An experimental approach, *Powder Technol.*, 415, 118176 (2023). https://doi.org/10.1016/j.powtec.2022.118176

Kumar, A., Hassan, M. A. and Chand, P., Heat transport in nanofluid coolant car radiator with louvered fins, *Powder Technol.*, 376, 631–642 (2020). https://doi.org/10.1016/j.powtec.2020.08.047

Lawal, S. A., Medupin, R. O., Yoro, K. O., Okoro, U. G., Adedipe, O., Abutu, J., Tijani, J. O., Abdulkareem, A. S., Ukoba, K., Ndaliman, M. B., Sekoai, P. T. and Jen, T. C., Nanofluids and their application in carbon fibre reinforced plastics: A review of properties, preparation, and usage, *Arab. J. Chem.*, 16(8), 104908 (2023). https://doi.org/10.1016/j.arabjc.2023.104908

Li, D., Liu, C., Chen, S., Kong, W., Zhang, H., Wang, D., Li, Y., Chang, J. and Cheng, C., Simplified Compact Perovskite Solar Cells with Efficiency of 19.6% via Interface Engineering, *Energy Environ. Mater.*, 3(1), 5–11 (2020). https://doi.org/10.1002/eem2.12063

Miao, Z., Meng, X. and Liu, L., Improving the ability of thermoelectric generators to absorb industrial waste heat through three-dimensional structure optimization, *Appl. Therm. Eng.*, 228, 120480 (2023). https://doi.org/10.1016/j.applthermaleng.2023.120480

Nieh, H. M., Teng, T. P. and Yu, C. C., Enhanced heat dissipation of a radiator using oxide nano-coolant, *Int. J. Therm. Sci.*, 77, 252–261 (2014). https://doi.org/10.1016/j.ijthermalsci.2013.11.008

Pak, B. C. and Cho, Y. I., Hydrodynamic and heat transfer study of dispersed fluids with 445 submicron metallic oxide particles, *Exp. Heat Transf.,* 11(2), 151–170 (1998). https://doi.org/10.1080/08916159808946559

Ravi, T. S., Chellapilla, V. K. N. S. N. M., Jayakumar, S., Kiran, K. A. and Srinivas, V., Ethylene Glycol-Based Nanofluids – Estimation Of Stability And Thermophysical Properties, *Front. Heat Mass Transf.*, 15, 1-9(2020). https://doi.org/10.5098/hmt.15.7

Roy, A., Venkitaraj, K. P., Vigneshwaran, P., Saboor, S., Cuce, E. and Saxena, K. K., Enhanced convective heat transfer with Al2O3-water nanofluid in a PCM-based thermal energy storage system, *J. Energy Storage*, 97, 112853 (2024). https://doi.org/10.1016/j.est.2024.112853

Ruey, O. H., Mohd, E. I. W., Yapp, J. M., Rahman, K. M. M., and Khairul, A. M. M., Effects of natural-based SiO_2 nanocoolant on car radiator: Thermal profile, *Mater. Today, Proc.*, 66, 2734–2737 (2022). https://doi.org/10.1016/j.matpr.2022.06.505

Sundari, K. G., Asirvatham, L. G., Joseph, J. M. S., Manova, S., Sahu, M. and Jesse, A. M., Heat transfer studies using glycerin based nanocoolant for car radiator cooling applications, *Mater. Today, Proc.*, 47, 7045–7049 (2021). https://doi.org/10.1016/j.matpr.2021.06.104

Tam, L. M. and Ghajar, A. J., Transitional Heat Transfer in Plain Horizontal Tubes, *Heat Transf. Eng.*, 27(5), 23–38 (2006). https://doi.org/10.1080/01457630600559538

Zakaria, I. A., Mohamed, W. A. N. W., Azid, N. H. A., Suhaimi, M. A. and Azmi, W. H., Heat transfer and electrical discharge of hybrid nanofluid coolants in a fuel cell cooling channel application, *Appl. Therm. Eng.*, 210, 118369 (2022). https://doi.org/10.1016/j.applthermaleng.2022.118369